
ESC Congress 2014, Barcelona, Spain

30 August – 3 September 2014

EDITOR-IN-CHIEF

Thomas F. Lüscher

DEPUTY EDITORS

Jeroen J. Bax
Bernard J. Gersh
Gerhard Hindricks

Ulf Landmesser
Frank Ruschitzka
William Wijns

CONSULTING EDITORS

Joe Loscalzo
Frans Van de Werf

INTERNATIONAL ASSOCIATE EDITORS

Colin Baigent
Helmut Baumgartner
Paolo Camici
David Celermajer (AU)
Francesco Cosentino
Filippo Crea
John E. Deanfield
Stephanie Dimmeler
Gerasimos Filippatos
Keith A.A. Fox
Runlin Gao (Asia)
John Gorsan III (US)
John J.P. Kastelein
John J.V. McMurray

Christian Mueller
Barbara Mulder
Thomas Münzel
N. Brahmajee (US)
Stefan Neubauer
Udo P. Sechtem
Ajay M. Shah (UK)
Hiroaki Shimokawa (JP)
Jagmeet P. Singh (US)
Karen Sliwa (ZA)
Karl Swedberg
Stefano Taddei
Alec Vahanian
Salim Yusuf (Canada)

LOCAL ASSOCIATE EDITORS

Ronald Binder
Corinna Bruckhorst
Giovanni G. Camici
Firat Duru
Urs Eriksson
Volkmar Falk
Oliver Gämperli
Nils Kucher

Willibald Maier
Christian Matter
Fabian Nietlispach
Christian Schmied
Jan Steffel
Felix C. Tanner
Christian Templin
Bernd van der Loo

STATISTICS EDITOR

Rickey Carter

SENIOR CONSULTING EDITORS

John Camm
Diederick E. Grobbee
Tiny Jaarsma
Gerald Maurer

Patrick W. Serruys
Karin Sipido
Dirk van Veldhuisen
Christian J.M. Vrints

EDITORIAL OFFICE

European Heart Journal
The Zurich Heart House
Moussonstrasse 4
CH-8091 Zurich
Switzerland
Phone: +41 (0)44 634 5537/38
Fax: +41 (0)44 634 5530
Email: Eurheartj@usz.ch
Homepage: www.eurheartj.org

Managing Editors

Sam Rogers
Susanne B. Dedede
Amelia Meier-Batschelet
Andros Tofield (CardioPulse and People's Corner)

INTERNATIONAL EDITORIAL BOARD

William T. Abraham (US)	Mark A. Creager (US)	Richard Kobza (CH)	Raphael Rosenhek (AU)
Stephan Achenbach (DE)	Harry Crijns (NL)	Philippe Kolh (BE)*	Carlos E. Ruiz (US)
Stefan Agewall (NO)	Nicolas Danchin (FR)	Michel Komajda (FR)	Lars Rydén (SE)
Fernando Alfonso (ES)*	Isabel Deisenhofer (DE)	Stavros V. Konstantinides (DE)	François Schiele (FR)
Joseph S. Alpert (US)	Kenneth Dickstein (N)	Steen Dalby Kristensen (DK)	Gerhard Schuler (DE)
Giuseppe Ambrosio (IT)	Raffaele De Caterina (IT)	Henry Krum (UK)	Heribert Schunkert (DE)
Felicitia Andreotti (IT)	Bart De Geest (BE)*	Irene Lang (AT)	Markus Schwaiger (DE)
Stefan Anker (DE)	Pascal de Groote (FR)	Ulrich Laufs (DE)	Peter J. Schwartz (IT)
Elliott M. Antman (US)	Edo D. de Muinck (SE)	Christophe Leclercq (FR)	Christian Seiler (CH)
David Antoniucci (IT)	Carlo Di Mario (GB)	Adelino Leite-Moreira (PT)	Paul Sergeant (BE)
Eliosa Arbustini (IT)	Eric Eeckhout (CH)	Amir Lerman (US)	Thomas Hellmut Schindler (CH)
Paul W. Armstrong (CA)	Raimund Erbel (DE)	Eli I. Lev (IL)	Evgeny Shlyakhto (RU)
Dan Atar (NO)	Paul Erne (CH)*	Peter Libby (US)	Maarten Simoons (NL)
Johann Auer (AT)*	Cetin Erol (TU)	Gregory Y.H. Lip (GB)	Karin Sipido (BE)
Luigi P. Badano (IT)	Francisco Fernández-Avilés (ES)	Massimo Lombardi (IT)	Peter Sogaard (DK)
Emanuele Barbato (BE)	Roberto Ferrari (IT)	Russell V. Luepker (US)	Scott Solomon (US)
Thomas Bartel (AT)*	Andrea Frustaci (IT)	François Mach (CH)	Rudolf Speich (CH)
Joshua Barzilay (US)*	Valentin Fuster (US)	Winfried Maerz (DE)	Christodoulos Stefanadis (GR)
Jean-Pierre Bassand (FR)	Nazzareno Galie (IT)	Aldo Pietro Maggioni (IT)	Philippe Gabriel Steg (FR)
Eric Bates (US)	Xavier Garcia-Moll (ES)	Eduardo Marban (US)	Steven Steinhilber (CH)
Hans-Jürg Beer (CH)	Anthony H. Gershlick (GB)	Koon-Hou Mak (SG)*	Gregg W. Stone (US)
Emelia Benjamin (US)	Lorenzo Ghiadoni (IT)	Michael Marber (GB)	Isabella Sudano (CH)*
Daniel S. Berman (US)	Anselm Kai Gitt (DE)	V. Mareev (RU)	Corrado Tamburino (IT)
Michel E. Bertrand (FR)	Samuel Z. Goldhaber (US)	Barry Maron (US)	Luigi Tavazzi (IT)
Deepak L. Bhatt (US)	Paolo Golino (IT)	Gerald Maurer (AT)	Michal Tendera (PL)
Luigi M. Biasucci (IT)*	Lino Gonçalves (PT)	William McKenna (GB)	Stefan Toggweiler (CH)*
Giuseppe G.L. Biondi-Zoccai (IT)	Tommaso Gori (DE)*	Jawahar L. Mehta (US)	Gianni Tognoni (IT)
Christoph Bode (DE)*	Christopher Granger (US)	Bernhard Meier (CH)	Adam Torbicki (PL)
Eric Boersma (NL)	Daniel Gras (F)	Franz H. Messerli (US)	Dimitris Tousoulis (GR)
Lucas V.A. Boersma (NL)	Steven M. Haffner (US)	Gilles Montalescot (FR)	Panagiotis Vardas (GR)
Giovanni Boffa (IT)*	Michel Haïssaguerre (FR)	Christian Müller (CH)	Albert Varga (HU)
Robert O. Bonow (US)	Göran K. Hansson (SE)	Franz-Josef Neumann (DE)	Freek W.A. Verheugt (NL)
Giuseppe Boriani (IT)	Christian Hamm (DE)	Georg Nickenig (DE)	Renu Virmani (US)
Jeffrey Borer (US)	Gerd Hasenfuss (DE)	Markku S. Nieminen (FI)	Jens-Uwe Voigt (BE)
Michael Böhm (DE)	Adrian F. Hernandez (US)	Petros Nihoyannopoulos (UK)	Massimo Volpe (IT)
Somjit S. Brar (US)	Gerd Heusch (DE)	Steven E. Nissen (US)	Nico Van de Veire (BE)*
Eugene Braunwald (US)	Judith S. Hochman (US)	Uwe Nixdorff (DE)	Ron van Domburg (NL)*
Günter Breithardt (DE)	David R. Holmes, Jr (US)	Suzanne Oparil (US)	Arnold Von Eckardstein (CH)
Ole Breithardt (DE)	Kurt Huber (AT)*	Seung-Jung Park (KR)	Ron Waksman (US)
Pedro Brugada (BE)	Sabino Illiceto (IT)	Terje R. Pedersen (NO)	Lars Wallentin (SE)
Nico Bruining (NL)	Bernard Jung (FR)	Dudley Pennell (GB)	Johannes Waltenberger (DE)
Raffaele Bugiardini (IT)	Allan S. Jaffe (US)	Joep Perk (SE)	Christian Weber (DE)
Hans-Peter Brunner-La Rocca (NL)	Stefan James (SE)	Marc A. Pfeffer (US)	Peter Wenaweser (CH)
Robert M. Califf (US)	Stefan Janssens (BE)	Eugenio Picano (IT)	Petr Widimsky (CZ)
François Cambien (FR)	James L. Januzzi (US)	Fausto Jose Pinto (PT)	James T. Willerson (US)
Christopher Paul Cannon (US)	Gabriela Kania (CH)	Bertram Pitt (US)	Bryan Williams (GB)
Davide Capodanno (IT)*	Juan-Carlos Kaski (UK)	Piotr Ponikowski (PL)	Stephan Windecker (CH)
Edoardo Casiglia (IT)*	Adnan Kastrati (DE)	Ton Rabelink (NL)	Kai Wollert (DE)
Filip P. Casselman (BE)	Hugo Katus (DE)	Frank Rademakers (BE)	Zhihong Yang (CH)
Bernard R. Chaitman (US)	Philipp A. Kaufmann (CH)	Daniel J. Rader (US)	Seppo Ylä-Herttuala (FI)
John G.F. Cleland (GB)	Malte Kelm (DE)	Shahbudin Rahimtoola (US)	Cheuk-Man Yu (CN)
David J. Cohen (US)	Alexander Kharlamov (NL)*	Kausik Ray (UK)	José Luis Zamorano (ES)
Antonio Colombo (IT)	Spencer B. King III (US)	Flavio Ribichini (IT)	Andreas Michael Zeiher (DE)
Richard C. Conti (US)	Helmut U. Klein (US)	Paul M. Ridker (US)	
Leslie Cooper (US)	Juhani Knuuti (FI)	Walter Riesen (CH)	
Maria R. Costanzo (US)	Jon Kobashigawa (US)	Marco Roffi (CH)	

P1514 | BENCH**Mechanisms of increased oxygen radical formation in alcoholic cardiomyopathy in a mouse model of acetaldehyde overload and potential therapeutic approaches**

M. Brandt¹, S. Kroeller-Schoen¹, M. Oelze¹, J. Mueller¹, T. Isse², A. Daiber¹, T. Muenzel¹, P. Wenzel¹. ¹University Medical Center of Mainz, Cardiology/2nd Medical Clinic, Mainz, Germany; ²University of Occupational and Environmental Health, Department of Environmental Medicine and Occupational Health, Kitakyushu, Japan

Background: Growing evidence suggests, that NADPH-oxidases (NOX) are involved in the pathogenesis of ethanol related organ damage. We sought to investigate the role of NADPH oxidase derived superoxide in the development of alcoholic cardiomyopathy (ACM) using ALDH2^{-/-} mice as an animal model of acetaldehyde overload and whether pharmacologic or genetic ablation of NOX2 could beneficially influence the disease model.

Methods: Male B6, ALDH2^{-/-} and ALDH2^{-/-}NOX2/gp91phox^{-/-} were fed a 2% ethanol vs. liquid control diet. After 5 weeks, cardiac function was assessed with echocardiography, malondialdehyde levels in internal organs were measured by dot blot. NOX activity in cardiac membrane fractions was quantified by chemiluminescence, while the expression of NOX2 was assessed by WB. For in vitro studies, cardiomyocytes (CMs) were isolated from B6 mice via cannulation and retrograde perfusion of the aorta. Plated CMs were incubated in culture media containing increasing concentrations of ethanol (EtOH) or acetaldehyde (MeCHO) in the presence or absence of the NOX inhibitor apocynin. Subsequently, CM mitochondrial membrane potential and mitochondrial ROS production was assessed by automated cellular imaging using the fluorescent probes TMRM+ and MitoSOX.

Results: ALDH2^{-/-} fed the 2% ethanol diet displayed a significantly decreased LV systolic function compared to ALDH2^{-/-} fed the liquid control diet and to B6 mice. Furthermore, ethanol-fed ALDH2^{-/-} mice exhibited significantly increased levels of malondialdehyde in internal organs (highest in the heart), increased heart/body and lung/body weight ratios, significantly increased cardiac NOX activity and significantly increased expression of the NOX2 subunit p67phox and the NOX2 activator Rac1 compared to control fed ALDH2^{-/-} and B6 mice. These results were corroborated by in vitro studies: cultured CMs which incubated with media containing MeCHO showed significantly increased levels of mitochondrial ROS and significantly decreased mitochondrial membrane potential. Pharmacologic ablation of NOX in CMs exposed to MeCHO lowered mitochondrial ROS and partially preserved mitochondrial membrane potential. Finally, we subjected mice double negative for ALDH2 and NOX2/gp91phox to the ethanol diet for 5 weeks. Echo revealed that the additional lack of NOX2/gp91phox protects mice from the acetaldehyde-overload induced cardiomyopathy.

Conclusions: Our results in vitro and in vivo data show that NOX derived ROS contributes to the development of ACM. We further provide evidence that ablation of NOX-2 can beneficially influence the disease in vitro and in vivo.

P1515**P1516 | BENCH****Nav1.5 N-terminus is responsible for the Nav1.5 and Kir2.x reciprocal modulation**

M. Perez-Hernandez¹, M. Matamoros¹, M. Nunez¹, A. Barana¹, I. Amoros¹, D. Ponce-Balbuena², J. Jalife², J.L. Tamargo¹, R. Caballero¹, E. Delpon¹. ¹Complutense University of Madrid, Pharmacology, Madrid, Spain; ²University of Michigan, Center for Arrhythmia Research, Ann Arbor, United States of America

Purpose: It has been demonstrated that the N-terminal domain of Nav1.5 channels (Nter), a 132 aminoacids peptide, is able to increase the Nav1.5 current (INav1.5) density. Additionally, it is known that there is a reciprocal modulation of the expression of Nav1.5 and Kir2.1 and Kir2.2 channels. Thus, we tested whether Nter is able to increase the expression of Kir2.x channels.

Methods: Currents were recorded using the patch-clamp technique in Chinese ovary cells transiently transfected with wild-type or site directed mutated Nter, Kir2.1, Kir2.2, and Nav1.5 channels.

Results: Cotransfection of Nter with Kir2.1 and Kir2.2 channels significantly increased Kir2.1 current (IKir2.1) and IKir2.2 measured at -120 mV from -126±12 to -183±18 pA/pF (n=25, P<0.05) and from -72±9 to -114±13 pA/pF (n=22, P<0.05), respectively. Conversely, cotransfection of Nter with Kir2.3 channels, which did not bind to syntrophin with a high affinity as demonstrated in immunoprecipitation experiments, did not significantly modify IKir2.3. Nter did not increase the current density generated by Nav1.5 channels lacking their C-terminal PDZ domain (Nav1.5ΔPDZ). Noteworthy, Nav1.5ΔPDZ channels still co-immunoprecipitated with syntrophin. We identified in the Nter peptide a sequence which could act as a "PDZ-like" binding domain (18-RESLA) and we tested its involvement in the Nter "chaperon" effect by site directed mutagenesis. The results demonstrated that mutants of all residues, except p.S20A Nter, increased IKir2.x. To further confirm the role of Ser20, p.S20A Nav1.5 channels were cotransfected with either Kir2.1 and Kir2.2 channels. Cotransfection of Kir2.1 channels with p.S20A Nav1.5 channels did not increase IKir2.1 as cotransfection with Nav1.5 channels did (from -126±12 to -192±16 pA/pF, n=35, p<0.05). Finally, to test the Nter chaperon effect in a cardiac model, adult rat ventricular myocytes were enzymatically dissociated, cultured, and infected with either a control adenoviral construction (Ad-GFP) or an Nter codifying adenoviral construction (Ad-Nter). Results demonstrated that myocyte infection with Ad-Nter significantly increased both the inward sodium (INa) and inward rectifier (IK1) currents.

Conclusions: The N-terminal domain of Nav1.5 channels exerts "chaperon-like" effect increasing INav1.5 and IKir2.x densities. This effect depends on the residue Ser20, which probably determines the binding to syntrophin via an "internal" PDZ binding domain.

P1517 | BENCH**Characteristics of pre-clinical models for the study of atherosclerosis and restenosis**

J.P. Hytonen, J. Taavitsainen, J.T.T. Laitinen, S. Tarvainen, O. Leppanen, S. Yla-Herttuala. A.I. Virtanen Institute for Molecular Sciences at the University of Eastern Finland, Kuopio, Finland

Purpose: Animal models are necessary for the evaluation of new endovascular therapies. We compared relevant models of restenosis with and without atherosclerotic injury in pigs and rabbits. Our aim was to compare the characteristics and feasibility of these models.

Methods: We compared atherosclerotic lesions induced by balloon injury and atherogenic diet in pig coronary arteries (n=33) and rabbit aorta (n=12). We also studied the lesions of WHHL rabbits (n=6), which portray a familial hypercholesterolemia type phenotype and have naturally high circulating cholesterol levels. In-stent restenosis (ISR) was also evaluated in different branches of the pig coronary tree by OCT imaging (n=12). Stents were implanted in the right (RCA), the left anterior descending (LAD) and left circumflex (LCX) coronary artery.

Results: Injured rabbit aortas developed lipid rich and uniform lesions. Porcine coronary injury produced lesions with varying characteristics and creation of lipid rich lesions was difficult even with high fat diet (picture). OCT follow up revealed very different characteristics in the different coronary branches in regards to the formation of in-stent restenosis. The RCA was found most resistant to ISR (RCA 17.9±3.5% vs LAD 33.7±3.8% vs LCX 39.9±9.2%) six weeks after stent implantation.

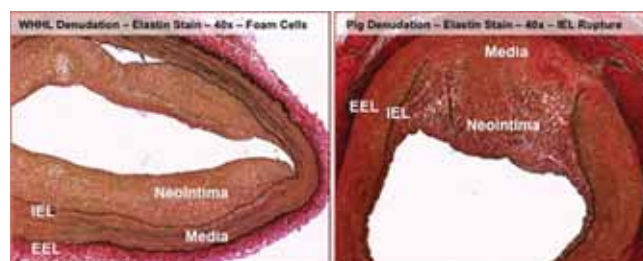


Figure 1. WHHL aorta and pig coronary histology.

Conclusions: The rabbit aorta with double injury of high cholesterol and mechanical de-endothelialization produced most atherosclerosis-like lesions. The

ABSTRACT WITHDRAWN

to express an inhibitory Gi-protein-coupled Drosophila allatostatin receptor (AlstR). Application of the AlstR ligand – the insect peptide allatostatin (5 μ M) produced rapid and reversible silencing of targeted vagal preganglionic neurones. These were targeted with two stereotaxic microinjections of a viral suspension containing either PRSx8-AlstR-eGFP-LV or PRSx8-eGFP-LV control.

Results: Activation of neurones in the left caudal DVMN resulted in a significant load-independent decrease in LVdP/dt max by -692 ± 193 mmHg/s ($n=11$, $p<0.0025$). This effect was abolished following intravenous administration of atropine methyl nitrate (2mg/kg, $n=7$). Acute inhibition of the DVMN neurones expressing AlstR following application of allatostatin resulted in a significant increase in LVdP/dt max by 922.3 ± 193 mmHg/s ($n=6$, $p<0.001$).

Conclusion: The data obtained challenges the prevailing view which persists in both the scientific and educational literature that the vagal innervation of the ventricle is sparse and insignificant. We demonstrate direct load- and heart rate-independent tonic control of ventricular contractility by a distinct population of vagal preganglionic neurones.

P2527 | BENCH

miR-208a/b decreases cardiac L-type Ca²⁺ current by targeting CACNA1C and CACNB2 mRNA

A. Barana¹, I. Amoros¹, M. Perez-Hernandez¹, M. Matamoros¹, M. Nunez¹, S. Canon², A. Bernad², J.L. Tamargo¹, E. Delpon¹, R. Caballero¹.

¹Complutense University of Madrid, Pharmacology, Madrid, Spain; ²National Centre for Cardiovascular Research (CNIC), Madrid, Spain

Purpose: Recent evidence have demonstrated that microRNAs, small non-coding RNA that regulate expression of target mRNA by binding to their 3'-untranslated regions (3'-UTR), can be partially responsible of the atrial fibrillation (AF)-induced electrical remodelling. Among them, microRNA-208a (miR-208a) and miR-208b are cardiac-specific microRNAs. It was demonstrated that miR-208b expression increases in right atrial appendages of AF patients. Since reduction of L-type Ca²⁺ current (I_{Ca,L}) density is a hallmark of the electrical remodelling, the aim of the present study was to determine whether miR-208a and miR-208b modulate I_{Ca,L}.

Methods: I_{Ca,L} was recorded at room temperature using Ba²⁺ as charge carrier (I_{Ba}) in HL-1 cells transfected or not with miR-208a and miR-208b mimics (at a final concentration of 30 nM) by whole-cell patch-clamp.

Results: Neither miR-208a nor miR-208b modified cell size as assessed by cell capacitance measurement (48.6 ± 8.7 and 39.8 ± 9.9 vs 34.7 ± 2.0 pF; $P>0.05$). Under control conditions, maximum I_{Ba} density was reached at +20 mV (-5.9 ± 1.0 pA/pF). miR208a and miR208b decreased peak I_{Ba} density at potentials positive to +10 (-2.2 ± 0.4 pA/pF for miR208a and -1.8 ± 0.3 pA/pF for miR208b at +20 mV; $P<0.01$ vs control). None of these microRNAs modified the voltage dependence of activation and inactivation. Importantly, a negative control miRNA failed to modify I_{Ba}, demonstrating the specificity of the observed effects. Bioinformatic algorithms such as miRanda and TargetMiner predicted that 3'UTR of both $\alpha 1C$ (CACNA1C) and $\beta 2$ (CACNB2), but not $\alpha 2\delta$ (CACNA2D) subunits can be targeted by miR-208a and miR-208b. These predictions were confirmed by luciferase reporter assays demonstrating that miR-208a and miR-208b produced a concentration-dependent decrease in the luciferase activity in CHO cells transfected with CACNA1C and CACNB2 3'UTR regions.

Conclusions: These results suggest that miR-208a and miR-208b may contribute to the development of AF-induced electrical remodelling, by means of a reduction of I_{Ca,L}.

P2528 | BEDSIDE

Association of genetic variants of the phosphatase and actin regulator 1 gene (PHACTR1) and the CDKN2B antisense RNA 1 (CDKN2BAS1) with coronary heart disease in Japanese individuals

R. Matsuoka¹, S. Abe¹, F. Tokoro¹, M. Arai¹, T. Noda¹, S. Watanabe¹, T. Fujimaki², M. Oguri³, K. Kato⁴, Y. Yamada⁵. ¹Gifu Prefectural General Medical Center, Department of Cardiology, Gifu, Japan; ²Inabe General Hospital, Department of Cardiovascular Medicine, Inabe, Japan; ³Nagoya First Red Cross Hospital, Department of Cardiology, Nagoya, Japan; ⁴Meitoh Hospital, Department of Internal Medicine, Nagoya, Japan; ⁵Mie University, Department of Human Functional Genomics, Life Science Research Center, Tsu, Japan

Purpose: Although various loci and genes that confer susceptibility to coronary heart disease (CHD) or myocardial infarction (MI) have been identified for Caucasian populations in genome-wide association studies (GWASs), genetic variants related to these conditions in Japanese individuals have not been identified definitively. The purpose of the present study was to examine a possible association of CHD or MI in Japanese with 15 polymorphisms identified as susceptibility loci for these conditions in the previously GWASs.

Methods: Study subjects comprised 4746 Japanese individuals (2462 subjects with CHD including 1822 with MI, 2284 controls) who visited the participating hospitals between 2002 and 2012. We selected 15 polymorphisms (each with a minor allele frequency of ≥ 0.05 in Japanese) reported by the previous GWASs for CHD or MI. Genotypes of polymorphisms were determined by the multiplex bead-based Luminex assay. To compensate for multiple comparisons, we adopted the criterion of a false discovery rate (FDR) of <0.05 for statistical significance of association.

Results: Comparisons of allele frequencies for 2462 subjects with CHD and 2284 controls by the chi-square test revealed that the rs9369640 of the phosphatase and actin regulator 1 gene (PHACTR1) ($P=0.00001$, FDR = 0.0002) and rs4977574 of the CDKN2B antisense RNA 1 (CDKN2BAS1) ($P=0.0042$, FDR = 0.0315) were significantly associated with CHD. Multivariable logistic regression analysis with adjustment for age, sex, body mass index, smoking status, and the prevalence of hypertension, diabetes mellitus, and dyslipidemia revealed that the rs9369640 ($P=0.0006$; odds ratio, 0.73; dominant model) and rs4977574 ($P=0.0043$; odds ratio, 1.26; recessive model) were significantly associated with CHD. The minor C allele of rs9369640 was protective against CHD, whereas the minor G allele of rs4977574 was a risk factor for this condition. Next, a relation of 15 polymorphisms to MI was examined among 1822 subjects with MI and 2284 controls. Comparisons of allele frequencies by the chi-square test revealed that the rs9369640 of PHACTR1 ($P=0.00002$, FDR = 0.0003) and rs4977574 of CDKN2BAS1 ($P=0.0003$, FDR = 0.0019) were significantly associated with MI. Multivariable logistic regression analysis with adjustment for covariates revealed that the rs9369640 ($P=0.0005$; odds ratio, 0.70; dominant model) and rs4977574 ($P=0.0004$; odds ratio, 1.37; recessive model) were significantly associated with MI.

Conclusions: The rs9369640 of PHACTR1 and rs4977574 of CDKN2BAS1 may be susceptibility loci for CHD and MI in Japanese individuals.

COMPUTED TOMOGRAPHY IN ASYMPTOMATIC HIGH RISK SUBJECTS

P2530 | BEDSIDE

Is metabolic syndrome predictive of coronary artery disease burden, and prognosis beyond its individual components? Results from the CONFIRM Registry

A. Ahmadi¹, J. Min², A. Berger³, B. Precious³, S. Achenbach⁴, B. Chow⁵, J. Hausleiter⁶, P. Kaufmann⁷, L. Shaw⁸, J. Leipsic³ on behalf of CONFIRM investigators. ¹University of British Columbia, Cardiology, Vancouver, Canada; ²Weill Cornell Medical College, Cardiology, New York, United States of America; ³University of British Columbia, Radiology, Vancouver, Canada; ⁴Justus-Liebig University of Giessen, Cardiology, Giessen, Germany; ⁵Ottawa Heart Institute, Cardiology, Ottawa, Canada; ⁶University Hospital of Munich, Cardiology, Munich, Germany; ⁷University of Zurich, Radiology, Zurich, Switzerland; ⁸Emory University School of Medicine, Cardiology, Atlanta, United States of America

Background: Metabolic Syndrome (MetS) is shown to increase the risk of cardiovascular disease and mortality. However, it is not yet known if MetS has any additive prognostic value beyond its individual risk factors (RF). The purpose of this study is to compare the prevalence, severity of coronary artery disease (CAD) and prognosis of patients with and without MetS.

Methods: The study cohort consisted of 27,125 consecutive individuals who underwent 64 detector row CCTA at 12 centers from 2003 to 2009. Patient with known CAD, unknown statin use or unavailable lipid profile were excluded. MetS was defined as per NCEP/ATP III criteria. We focused on 3900 patients who had measured RF for MetS and were not on statin therapy. Of these, 690 patients met the diagnostic criteria for MetS. Propensity matching was performed for age, sex, smoking status and family history of premature CAD with patients without MetS (no-MetS) with 0, 1, or 2 MetS RF. CAD was defined as none, non-obstructive (1–49% stenosis), or obstructive ($\geq 50\%$ stenosis). Major adverse cardiac events (MACE) was defined as MI, acute coronary syndrome, all cause mortality and late revascularization. MACE was assessed by risk-adjusted Cox proportional hazards models.

Results: MetS group had higher rates of obstructive 1, 2 and 3-vessel/left main disease compared to no-MetS group with 0 or 1 RF (13.8 vs. 8.8%, 4.5% vs. 2.4% and 2.3% vs. 0.9%, respectively; $p<0.01$). However, presence of obstructive 1, 2 and 3-vessel/ left main disease was not significantly different between MetS and no-MetS group with 2 RF (13.8 vs 10.5%, 4.5% vs 2.8% and 2.3% vs 1.3%, respectively; $p=$ non significant (NS)). At 2.2 year follow up, MetS group had higher MACE compared to no-MetS subgroups with 0 or 1 RF (4.4% vs 1.6%; $P<0.01$). There was no statistically significant difference in MACE between MetS group and no-MetS subgroup with 2 RF (4.4% vs 3.2% $P=NS$).

Conclusion: The prevalence and severity of CAD as well as MACE rate are significantly higher in MetS group compared to no-MetS group. However, these differences are not significant when comparing MetS group with no-MetS subgroup with 2 RF. These findings challenge the prognostic value of MetS as a syndrome beyond the sum of its components.

P2531 | BEDSIDE

Assessing the pretest probability of obstructive coronary disease - can we afford to ignore the cardiovascular risk factors?

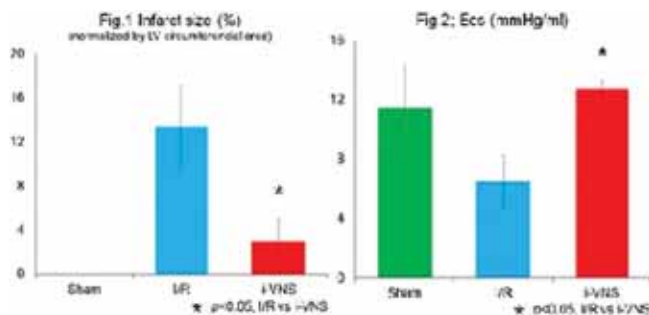
A. Silva Ferreira¹, P. Goncalves¹, M.B. Santos², H. Dores², M.S. Carvalho², A. Tralhao², S. Madeira², A. Damasio³, N. Cardim¹, H. Marques¹. ¹Hospital Luz, Imaging Center, Lisbon, Portugal; ²Hospital Santa Cruz, Centro Hospitalar Lisboa Ocidental, Lisbon, Portugal; ³Hospital Espirito Santo de Evora, Cardiology, Evora, Portugal

Background: The European Society of Cardiology (ESC) 2013 Guidelines on

VNS has been shown to exert powerful anti-infarct effects, the technical difficulty associated with VNS precludes its application under emergent settings of AMI. In this study, we developed a novel technique of intravenous VNS and evaluated how the VNS affects the infarct size and cardiac function 4 weeks after AMI with reperfusion.

Method: In 11 mongrel dogs, we ligated a left anterior descending coronary artery for 3 hours, then reperfused. For the intravenous VNS, we performed the field electrical stimulation between a pacing catheter in the superior vena cava and an electrode pad attached to the back. We delivered VNS from the beginning of ischemia to 1 hour after reperfusion. We titrated the strength of VNS to lower heart rate by 20–30%. We divided animals into 3 groups, sham operation/no stimulation (Sham, N=3), ischemia-reperfusion (I/R, N=4), and I/R+VNS (I/R-VNS, N=4). 4 weeks after ischemia, we evaluated hemodynamics and left ventricular function in terms of end-systolic elastance (Ees). We also histologically estimated the infarct size.

Results: During operation, mean heart rate were significantly lower in I/R-VNS than in I/R (107 ± 20 vs. 134 ± 16 bpm, $p < 0.05$), while blood pressure didn't differ among 3 groups. I/R-VNS strikingly decreased the infarct size more than 80% ($p < 0.05$, Fig. 1) and improved Ees ($p < 0.05$, Fig. 2). I/R-VNS markedly decreased left ventricular end-diastolic pressure (5.0 ± 1.6 vs. 23.8 ± 2.5 mmHg, $p < 0.05$) and serum NT-pro BNP (843 ± 256 vs. 3667 ± 1637 pmol/ml, $p < 0.05$).



The effect of VNS for infarct size & Ees.

Conclusion: Intravenous VNS in AMI markedly reduces the infarct size and improves cardiac function in the chronic phase.

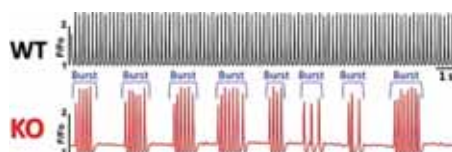
P5360 | BENCH

Funny current mediated pacemaker activity in the sinoatrial node of sodium-calcium exchanger knockout mice

A.G. Torrente¹, A. Zaini¹, A. Rosenberg¹, R. Zhang¹, J. Kang¹, K.D. Philipson², J.I. Goldhaber¹. ¹Cedars-Sinai Medical Center, Heart Institute, Los Angeles, United States of America; ²University of California Los Angeles, Department of Physiology, David Geffen, Los Angeles, United States of America

Purpose: The sodium-calcium exchanger (NCX) is the major Ca extruder of myocytes. In the sinoatrial node (SAN) both NCX and funny current (If) participate in the depolarization that initiates pacemaker activity. To clarify the relative contribution of NCX to SAN pacing, we created an atrial-specific NCX knockout (KO) mouse. This mouse does not express any NCX in the atrial region, including the SAN. Phenotypically, NCX KO mice lack P waves on their electrocardiograms and have quiescent isolated SAN cells. Recording the Ca dynamics in a novel preparation that includes the SAN and atria, we investigated whether atrial remodelling may have obscured residual pacemaker activity in NCX KO SAN tissue.

Methods and results: Using high speed 2D confocal microscopy we found that the KO SAN exhibited bursts of organized Ca transients alternating with pauses, characterized by abundant intracellular Ca waves. Although, the overall rate of Ca transients in NCX KO SAN (~2Hz; n=25) was reduced by the numerous pauses, the frequency of Ca transients during the bursts was rapid. Their average frequency (~4Hz; n=24) was not significantly different from WT (~5Hz; n=24). When considering only the rate during the burst, we found that 6 out of 10 KO SANs responded significantly to β -adrenergic stimulation (isoproterenol $10 \mu\text{M}$; $52 \pm 16\%$ rate increase). This response was smaller but still comparable to the increase in WT SANs ($70 \pm 6\%$; n=5). The pacemaker activity of both genotypes responded to the If blocker ivabradine (IVA, $9 \mu\text{M}$). At higher doses of IVA ($27 \mu\text{M}$) WT SANs decreased their rate by $43 \pm 4\%$, while KO SAN Ca transients were effectively eliminated.



Ca transients generated by the SAN.

Conclusions: These results indicate that If generates the burst pacemaker activity found in the NCX KO SAN, and allows the partial β -adrenergic responsiveness of the KO.

P5361 | BENCH

Pitx2 decreases L-type Ca²⁺ current and increases the slow delayed rectifier K⁺ current in cardiac cells

M. Nunez¹, I. Amoros¹, M. Matamoros¹, M. Perez-Hernandez¹, A. Barana¹, D. Franco², J.L. Tamargo¹, E. Delpon¹, R. Caballero¹. ¹Complutense University of Madrid, Pharmacology, Madrid, Spain; ²University of Jaen, Jaen, Spain

Purpose: Genome wide scan analyses demonstrated that single nucleotide polymorphisms in the human chromosome 4q25, proposed to regulate the activity of the adjacent transcription factor Pitx2, were associated with an increased risk in atrial fibrillation (AF). Recent evidence has shown that Pitx2 could play a role in AF-induced electrical remodelling. However, its putative role in the control of expression/function of the ion channels responsible for atrial action potential is currently unknown. This work was undertaken to determine the effects of Pitx2 on voltage-gated cardiac Ca²⁺ and K⁺ channels.

Methods: Currents were recorded in HL-1 cells transfected or not with the cardiac Pitx2 isoform (Pitx2c) by using whole-cell patch-clamp. L-type calcium current (ICa,L) was recorded by using Ba²⁺ as charge carrier (IBa).

Results: Under control conditions, peak IBa density was reached at +20 mV (-4.6 ± 0.6 pA/pF). Pitx2c significantly reduced peak IBa density (-2.8 ± 0.3 pA/pF at +20 mV, $p < 0.05$) without modifying activation, inactivation, and reactivation kinetics or voltage-dependent activation and inactivation. Regarding voltage-gated K⁺ channels, under control conditions 2 groups of cells were identified based on the predominant voltage-gated K⁺ current exhibited. In most of the cells (~80%), a rapid delayed rectifier current (IKr) sensitive to dofetilide could be recorded, which reached a mean density of 1.9 ± 0.2 pA/pF at 0 mV. In the rest of the cells (~20%), IKr was absent and the predominant current was a fast activating and slow inactivating outward current sensitive to 4-aminopyridine (2 mM), with biophysical properties compatible with the ultrarapid delayed rectifier K⁺ current (IKur) recorded in human atrial myocytes. In the presence of Pitx2c, only a small subset of the cells exhibited IKur (~10%) sensitive to 4-aminopyridine. Importantly, most of the cells (~90%) exhibited a voltage-gated, dofetilide-resistant, K⁺ current with a very slow activation kinetics (τ_{act} at +60 mV = 1.8 ± 0.3 s) that reached 8.9 ± 3.0 pA/pF after 5-s pulses to +60 mV. The mean midpoint of the activation curve was 20.0 ± 3.9 mV. This current was completely abolished by HMR-1556 ($1 \mu\text{M}$). All the biophysical and pharmacological properties of the Pitx2c-induced current resembled those of the human cardiac IKs.

Conclusions: The results demonstrated that Pitx2c decreased ICa,L and increased IKs and suggested that this transcription factor could contribute to the reduction of ICa,L and the increase of IKs that characterise the AF-induced electrical remodelling.

CARDIAC HYPERTROPHY AND HEART FAILURE

P5363 | BENCH

CTCF is prerequisite for the fetal gene expression in the process of hypertrophy of the cardiomyocyte

K. Iwai¹, T. Okuno¹, T. Morita¹, H. Yano¹, O. Iritani¹, M. Okuro¹, S. Morimoto¹, Y. Nakamura², Y. Ishigaki². ¹Geriatric Medicine, ²Medical Research Institute, Kanazawa Medical University, Kahoku-gun, Japan

Purpose: CCCTC-binding factor (CTCF) is a multifunctional chromatin modulator protein in the nucleus and regulates the phenotypic changes in differentiation or carcinogenesis in various types of cells. We hypothesized that CTCF is one of the master weaver of the cardiac genome and first investigated its roles in the fetal gene expression on the process of cardiac hypertrophy.

Methods: Neonatal rat cardiomyocytes (2-3 do) were cultured. CTCF mRNA was either knocked-down using siRNA or over-expressed by transfection with plasmid loading full-length CTCF cDNA. Hypertrophic stimulation were given by angiotensin II (All: 0.1 – $0.4 \mu\text{M}$) or norepinephrine (NE: $1 \mu\text{M}$) for 24hrs. Gene expression was investigated by real-time PCR analysis using SYBR-Green method. Microarray profiling analysis of mRNAs was performed.

Results: Immunofluorescence and western blot showed CTCF localized in the nuclei of the cardiomyocytes. Knocking down of CTCF mRNA ($-61 \pm 4\%$, n=4) suppressed the gene expression of both β -myosin heavy chain (β -MHC) ($-45 \pm 7\%$, $p < 0.01$) and α -skeletal actin (α -SA) ($-25 \pm 3\%$, $p < 0.01$). Pre-treatment with 5-Aza-2'-deoxycytidine ($2 \mu\text{M}$) cancelled these suppressive effects by knocking down of CTCF (n=3), indicating DNA methylation is involved in the function of CTCF. After stimulation with All or NE cell surface area was significantly increased, indicating hypertrophy occurred. Under knocking down of CTCF (n=8), up-regulation of β -MHC mRNA to $190 \pm 17\%$ following stimulation with All (n=4) was suppressed to $123 \pm 21\%$ ($p < 0.01$), and up-regulation of α -SA to $191 \pm 22\%$ was also suppressed to $108 \pm 9\%$ ($p < 0.01$). With NE (n=4) up-regulation of β -MHC to $155 \pm 24\%$ was suppressed to $51 \pm 7\%$ ($p < 0.01$), and up-regulation of α -SA to $159 \pm 23\%$ was also suppressed to $42 \pm 5\%$ ($p < 0.01$). On the other hand, only over-expression of CTCF (n=4) increased the gene expression of β -MHC to $204 \pm 18\%$ and α -SA to $134 \pm 17\%$ ($p < 0.01$). But, unexpectedly it suppressed the up-regulation of β -MHC to $110 \pm 12\%$ and α -SA to $106 \pm 11\%$ following stimulation with All ($p < 0.01$, n=4). The extent of α -MHC mRNA was not significantly changed after gain or loss of CTCF. Microarray profiling analysis after knocking down of CTCF demonstrated significant down-regulation of 56 genes including WNT1 inducible signaling pathway protein 2, and significant up-regulation of 50 genes including G-protein coupled receptor 37.